Full-Band Modeling of Mobility in p-Type FinFETs

Z. Stanojević*, O. Baumgartner*, M. Karner[†], Lª. Filipović*, C. Kernstock[†], and H. Kosina*

*Institute for Microelectronics, TU Wien, Gußhausstraße 27-29/E360, 1040 Vienna, Austria

[†]Global TCAD Solutions GmbH., Landhausgasse 4/1a, 1010 Vienna, Austria

Email: {stanojevic|baumgartner|lidijafilipovic|kosina}@iue.tuwien.ac.at, {m.karner|c.kernstock}@globaltcad.com

Tel. +43-1-58801-36016, FAX: +43-1-58801-36099

Abstract—We present a framework for modeling the low-field mobility of ultra-narrow Si channels such as FinFETs based on a full-band description of the electronic structure. Hole mobility is of particular interest since its calculation necessitates a full-band approach. Our approach is entirely based on physical modeling and thus naturally includes effects of gate field, crystal orientation, or strain.

MODELING APPROACH

Our modeling framework consists of three major parts: (i) self-consistent electronic structure calculation, (ii) linearized Boltzmann transport, and (iii) semiclassical scattering. The computational workflow is presented in Fig. 1.

1) Electronic Structure: We describe the electronic structure of the valence band in silicon using a $\mathbf{k} \cdot \mathbf{p}$-Hamiltonian [1]. The subband structure of the channel is obtained by discretizing the Hamiltonian in real space in the channel cross section. Calculating the subband structure involves solving an eigenvalue problem for each point on a $\mathbf{k}$-grid in the direction of free propagation.

2) Transport: Carrier transport in the semi-classical regime is described by the Boltzmann transport equation (BTE). Here, we are interested in the stationary case with a uniform electric field in transport direction. We assume that the distribution function $f_n(\mathbf{k})$ consists the equilibrium distribution f^0 plus a linear carrier response f^1, $f_n(\mathbf{k}) = f^0(E - E_F) + f_n^1(\mathbf{k})$. This results in the linearized Boltzmann transport equation (LBTE),

$$\sum_{n',\mathbf{k}'} S_{n,n'}(\mathbf{k}, \mathbf{k}')\big[f_n^1(\mathbf{k}) - f_{n'}^1(\mathbf{k}')\big] = -\mathbf{F} \cdot \mathbf{v}_n(\mathbf{k})\frac{\mathrm{d}f^0}{\mathrm{d}E}.$$

The LBTE is discretized in $\mathbf{k}$-space to obtain its discrete representation,

$$\sum_{\nu'} S_{\nu,\nu'} w_{\nu,\nu'}\big[f_\nu^1 - f_{\nu'}^1\big] = -\mathbf{F} \cdot \mathbf{v}_\nu\frac{\mathrm{d}f^0}{\mathrm{d}E}V_{\mathbf{k}},$$

where $\nu = (n, \mathbf{k})$ denotes the index of each state on the $\mathbf{k}$-grid in each subband. $S_{n,n'}(\mathbf{k}, \mathbf{k}')$ and $S_{\nu,\nu'}$ are the transition rates due to the various scattering processes described in the next section; $w_{\nu,\nu'}$ are weights that convert the transition rates to probability fluxes between the cells of the $\mathbf{k}$-grid as illustrated in Fig. 2. $V_{\mathbf{k}}$ is the volume of a $\mathbf{k}$-grid cell. Contrary to common practice [2], we avoid introducing a momentum relaxation time $\tau_n(\mathbf{k})$ in the LBTE. The momentum-relaxation-time-picture sacrifices information necessary to accurately capture anisotropic scattering processes. Instead, by solving directly for f^1, we treat anisotropic scattering correctly.

3) Scattering: Scattering processes are computed according to Fermi's golden rule. The following scattering processes dominant in ultra-narrow channels at room temperature are included: phonon scattering, ionized impurity scattering, and surface roughness scattering (SRS). SRS is treated using an extended Prange-Nee theory for non-planar structures developed in our previous works [3–5]. The key point of the theory is to replace the Prange-Nee *form factors* by *form functions*. The resulting transition rate reads

$$S_{n,n'}(\mathbf{k}, \mathbf{k}') = \frac{1}{2\hbar L}\int_{\mathbb{R}} |F_{n,n';\mathbf{k},\mathbf{k}'}(q_\perp)|^2 C(\mathbf{q})\mathrm{d}q_\perp,$$

where $F_{n,n';\mathbf{k},\mathbf{k}'}(q_\perp)$ are the Fourier transforms of the form functions - called *spectral form functions* - and $C(\mathbf{q})$ is the roughness power spectrum. Figs. 3 and 4 illustrate the process of obtaining the transition rate.

RESULTS

We present a study of hole mobility in p-type Si FinFETs with different channel and substrate orientations. The hole concentration profile is shown in Fig. 5. The investigated channel/substrate orientations are $\langle 100\rangle/\{100\}$, $\langle 110\rangle/\{100\}$, and $\langle 110\rangle/\{110\}$. Channel mobility was computed for various gate voltages and is displayed as function of inversion density in Fig. 6. There are significant differences in the mobility curves of the different orientations with $\langle 110\rangle/\{110\}$ exhibiting the best and $\langle 100\rangle/\{100\}$ the worst transport properties. All models were implemented within the Vienna Schrödinger-Poisson simulation framework [6].

CONCLUSION

We developed a comprehensive set of computational methods for physical modeling of non-planar, ultra-narrow channels such as FinFETs. The modeling relies on a $\mathbf{k} \cdot \mathbf{p}$-based electronic structure calculation and linearized Boltzmann transport with semiclassical scattering. A study of the channel mobility in p-type Si FinFETs, where mobility exhibits significant orientation dependence, highlights the importance of such physical modeling for ultra-narrow p-type channels.

ACKNOWLEDGMENT

REFERENCES

[1] T. Manku *et al.*, J. Appl. Phys. **73**, 1205 (1993).
[2] M. V. Fischetti *et al.*, Journal of Applied Physics **94**, 1079 (2003).
[3] Z. Stanojevic *et al.*, *Silicon Nanoelectronics Workshop* (2013), pp. 132–133.
[4] Z. Stanojevic *et al.*, *Intl. Conf. on Simulation of Semiconductor Processes and Devices* (2013), pp. 352–355.
[5] Z. Stanojevic *et al.*, *Intl. Electron Device Meeting* (2013).
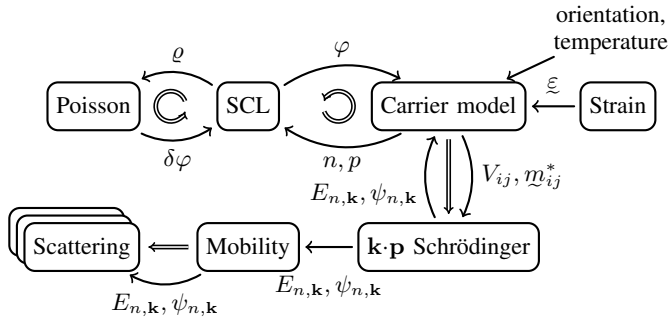[6] http://www.globaltcad.com/en/products/vsp.html.

Fig. 1. A self-consistent loop (SCL) is used to obtain potential and carrier concentration. The subbands and wavefunctions from the converged iteration are then used in the mobility model and the scattering models to compute scattering rates, probability fluxes, and finally the channel mobility.
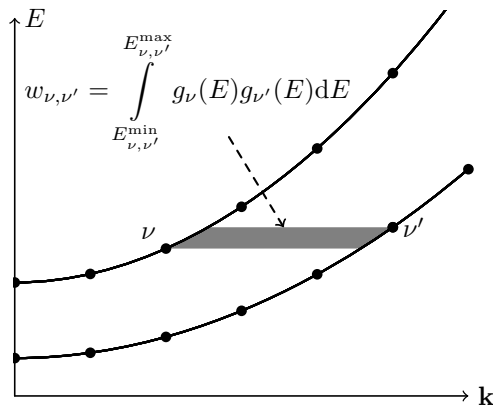

Fig. 2. Calculation of the coupling weights for the LBTE; $w_{\nu,\nu'}$ is obtained by integrating the product of the density of states of state ν and ν' over the energy interval where ν and ν' overlap. Multiplied by a scattering rate it gives the probability flux between ν and ν'.
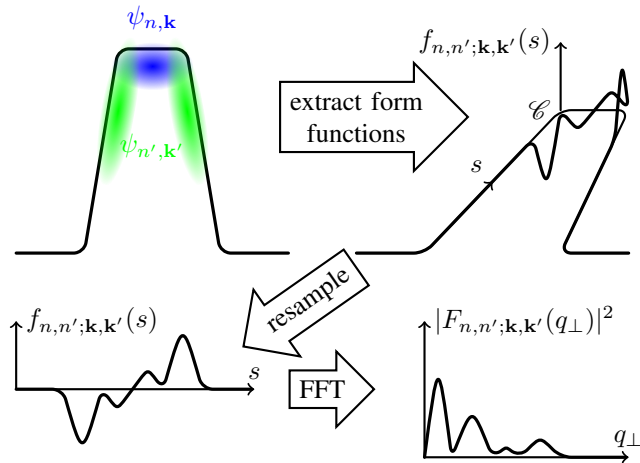

Fig. 3. Illustration of the calculation of the *spectral form function* between two states $n, \mathbf{k}$ and $n', \mathbf{k}'$ in a FinFET cross-section; the form functions are computed along the surface/interface path $\mathscr{C}$ analogous to the form factors in the Prange-Nee model. The form function is shown as function of the path coordinate s. Its Fourier transform gives the *spectral form function*.
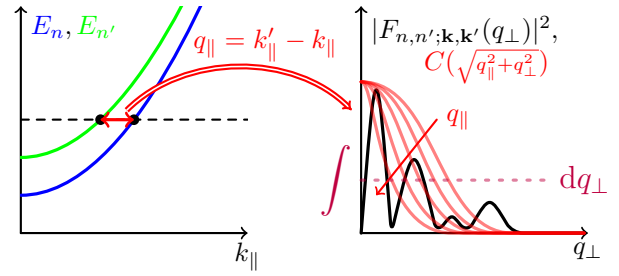

Fig. 4. The product of spectral form function and lateral roughness spectrum is integrated to obtain the transition rate. The shape, i.e. the band-width, of the lateral roughness power spectrum is determined by the longitudinal momentum transfer.
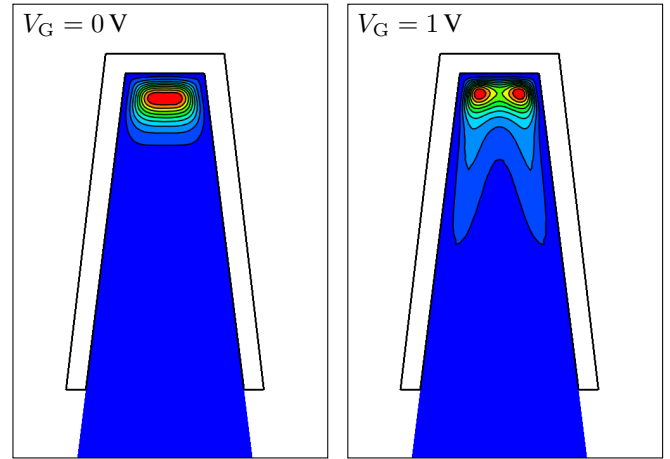

Fig. 5. Hole concentration profile at low (left) and high (right) inversion for channel/substrate orientation $\langle 100 \rangle / \{100\}$; the holes exhibit true two-dimensional confinement in the channel, and are centered below the fin top at low inversion densities. At high inversion densities the holes form regions of quasi-one-dimensional inversion near the sidewalls.
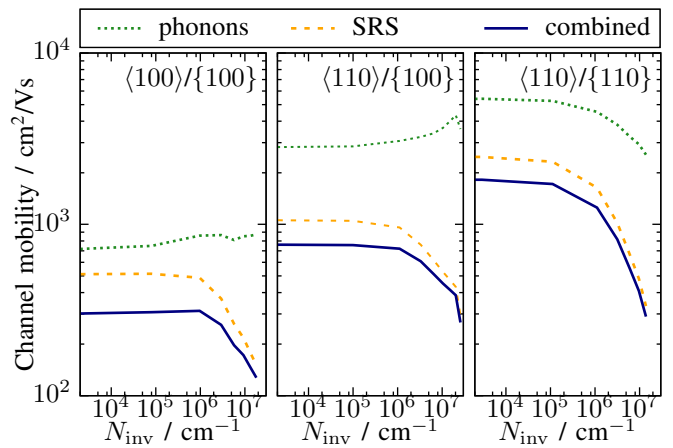

Fig. 6. Mobility vs. hole inversion density; $\langle 100 \rangle / \{100\}$ channel mobility is below $\langle 110 \rangle / \{110\}$. Mobility is mostly limited by SRS which causes all three curves to decrease at high inversion densities. Interestingly, phonon-limited mobility increases slightly for $\langle 100 \rangle / \{100\}$ and the $\langle 110 \rangle / \{100\}$ channel due to energy-separation of the heavy and light hole bands by the gate field.